Experimental study on air pressure variation in a horizontal pipe of single-stack drainage system

Tingchao Yu, Qiang Ding, Luwen Wang, David Z. Zhu and Yu Shao

ABSTRACT

The water trap seal under the sanitary appliances is the primary defense against the ingress of foul gases and odors. However, research on air pressure variation in a horizontal pipe of a single-stack drainage system is very limited. Thus a physical model study was conducted to investigate the air pressure variation in a horizontal pipe. Four parameters were studied that affect the pressure variation; that is, water flow rate, inlet height, ventilation condition and outlet condition. When the top of the vertical drainage stack and the outlet were fully open to the atmosphere, the flow in the horizontal pipe changed from free surface flow to slug flow at certain times. The mean values and magnitudes of pressure fluctuation at measuring points on the horizontal pipe increased with Q_w but decreased along the horizontal pipe. The inlet height had relatively small influence on the pressure variation. Three ventilation conditions; that is, top fully open, half open and sealed, were tested, and a choking flow was formed in the vertical drainage stack and the pressure in the horizontal pipe decreased under the top sealed condition. Three outlet conditions; that is, outlet fully open, half submerged and fully submerged, were tested. The pressure in the horizontal pipe increased significantly under the outlet fully-submerged condition, which should be avoided in the actual operation by careful designing.

Key words | horizontal pipe, inlet height, outlet condition, pressure, ventilation condition, water flow rate

Tingchao Yu
Qiang Ding
Luwen Wang
David Z. Zhu
Yu Shao (corresponding author)
Department of Civil Engineering,
Zhejiang University,
Hangzhou 310058,
China
E-mail: *shaoyu1979@zju.edu.cn*

Qiang Ding
David Z. Zhu
Department of Civil and Environmental Engineering,
University of Alberta,
Edmonton, AB,
Canada,
T6G 2W2

NOTATION

The following symbols are used in this paper:

A_1 Cross-sectional area of air pocket
A_2 Cross-sectional area of water column
D_i Diameter of inflow branch pipe
D_s Diameter of vertical drainage stack and horizontal pipe
g Gravitational acceleration
H Inlet height
h_1 Height of air pocket
h_2 Elevation of water surface
l_1 Length of air pocket
l_2 Length of water column
$Q*$ Dimensionless water flow rate $Q^* = Q_w/(gD_s{}^5)^{1/2}$
Q_a Air flow rate
Q_w Water flow rate
x The distance from the measuring point to the vertical drainage stack
ρ Water density

doi: 10.2166/wst.2019.014

INTRODUCTION

The basic function of a building drainage and vent system is to rapidly carry away sewage discharged from sanitary appliances while prevent foul gases and odors from diffusing into residents' houses (Swaffield & Campbell 1992; Swaffield *et al.* 2004a). In low-rise buildings (up to six floors), single-stack drainage systems are widely used, in which air is

supplied through the top of the vertical drainage stack and mixed with water together flowing down. In mid-rise or higher buildings (above seven floors), a vent stack parallel to the vertical drainage stack is used separately for air supply, which is helpful to keep a good pressure balance and control pressure fluctuation but is more complicated to build and maintain (Cheng *et al.* 2008a).

In single-stack drainage systems, sewage is gathered and discharged from sanitary appliances into drainage branch pipes initially and then falls into a vertical drainage stack. After that, the sewage is discharged into a pipe with a relatively low slope (for simplicity of expression and distinction from the vertical pipe, such pipes are called horizontal pipes) and drained away. During this process, the water trap seal under the sanitary appliances is the primary defense against the ingress of foul gases and odors to prevent possible infection risk. Once the water trap seal is broken by pressure fluctuation, the faulty performance of building drainage and vent systems would not only cause inconvenience as a result of foul gases and odors, but also pose risks to human health by transporting infectious diseases into habitable space inside a building. In the case at the Amoy Gardens housing complex in Hong Kong, with the massive outbreak of a SARS (Severe Acute Respiratory Syndrome) epidemic in early 2003, the functional failure of a water trap seal introduced a potential route for the transmission of contaminated fecal droplets to other living spaces inside the building (Kay *et al.* 2006; Cheng *et al.* 2008b; Kelly *et al.* 2008a, 2008b).

The water trap seal was invented in the 18th century and has dominated the development of building drainage and vent systems since the 1850s (Swaffield *et al.* 2004a, 2004b). It is typically a U-tube manometer that responds to pressure variations in the building drainage and vent system. A normal water trap seal depth is about 50 to 75 mm depending on the appliance type and locations. As specified by relevant European and other international standards, a pressure fluctuation not exceeding some ±375 Pa might be tolerated in the building drainage and vent system (Swaffield & Campbell 1992; Swaffield *et al.* 2004a). The pressure variation that leads to water trap seal failure can be affected by many factors, such as water flow along the pipeline, air supply from the top of the stack and improper conditions outside the outlet (Cheng *et al.* 2008b). The random discharge of appliances upstream could result in a complex flow regime and pressure variation inside the building drainage and vent system. When the waste water flows down along the vertical drainage stack, air in the pipeline could be entrained resulting in a pressure reduction due to the moment transfer between the water phase and air phase (Ma *et al.* 2016). Swaffield & Thancanamootoo (1991) indicated that the annular water flow along the sidewall of the building drainage stack would generate air pressure that caused trap seal siphonage. Swaffield & Campbell (1992) investigated the effect of fluctuating air pressure in the vertical drainage stack upon the water trap seal. They analyzed the unsteady propagation of transient air pressure, and demonstrated the relationship between appliance discharge and the subsequent propagation of air pressure transients within both the vertical drainage stack and the associated vent network. A number of studies modelled the positive or negative air pressure transient. Swaffield & Jack (1998) provided generally applicable mathematical expressions to determine the pressure regime from experimental testing of several single-stack systems. The water trap seal can therefore be depleted by either excessive negative pressure sucking the trap seal water down into drainage pipe or excessive positive pressure forcing the trap seal water up into the sanitary appliance (Swaffield & Jack 2004; Swaffield *et al.* 2004b). Cheng *et al.* (2005, 2008a) focused on an empirical approach to air pressure prediction in a vertical drainage stack, given single point discharge and steady flow condition.

According to previous studies, the depletion of the water trap seal is mainly about the pressure variation in the vertical drainage stack, but the pressure variation in the downstream horizontal pipe is relatively less studied correspondingly. Most studies focused on the movement of water and air in municipal drainage pipes. Wang *et al.* (2012) investigated the air flow through gravity sewer airspaces. Qian *et al.* (2018) regarded the dropshaft as the key contribution for the pressure variation of the downstream sewer pipe. Wei *et al.* (2018) conducted an experiment to investigate the influence of pressurized downstream condition on the air pressure and air circulation in the dropshaft. They proposed an 'effectiveness factor' to measure the effectiveness of the internal air circulation on reducing the outside air entrainment. Huang *et al.* (2018) conducted a large-scale experimental study of geysers through a vent pipe connected to flowing sewers. They found that the transient pressure was about three times the driving pressure head. Li & Zhu (2018) presented a numerical analysis of flow processes associated with the pressurization and release of an air pocket in order to study its influence on transient pressure in a horizontal pipe with an end orifice. Therefore, it is of great interest to combine the influence of the vertical drainage stack with the pressure variation in the horizontal pipe. Besides,

there is still lack of knowledge on the effect of ventilation condition on the pressure variation in the horizontal pipe. Ding & Zhu (2018) investigated the flow regimes in a dropshaft with limited air supply. The ventilation condition of the dropshaft top could significantly affect the flow regime and pressure variation in the dropshaft. Model scales have been found to be important for studying the air entrainment process. Stephenson & Metcalf (1991) and Chanson (2009) found that the air entrainment in a small-scale model significantly underestimated that in the prototype. In a real building drainage and vent system, the peak of water consumption or sudden torrential rainfall may cause the horizontal pipes to be overloaded and the outlet becomes submerged. This situation would also affect the pressure variation in the horizontal pipe. In this study, the pressure characteristics in a horizontal pipe were discussed. Four parameters affecting the pressure variation; that is, water flow rate, inlet height, ventilation condition and outlet condition, were studied. The relative air flow rate was also measured in the experiments.

EXPERIMENTAL SETUP

Single-stack building drainage systems are usually used in buildings less than 7 floors in height, for which the diameters of vertical and horizontal drainage pipes are commonly 75 mm and 100 mm. Compared with the actual drainage pipes and the limitation of the experimental conditions, a 50 mm pipe is used for both the vertical drainage stack and the downstream horizontal pipe in this study. A transparent plexiglas model composed of an upstream inflow branch pipe, a vertical drainage stack and a downstream horizontal pipe was set up to simulate a single-stack drainage system, as shown in Figure 1. The upstream horizontal inflow branch pipe was 1.00 m long and its diameter (D_i) was 0.025 m. The height of the vertical drainage stack was 2.50 m with a diameter (D_s) of 0.050 m. Four inlet heights (H) at 0.5 m, 1.0 m, 1.5 m and 2.0 m were studied to see their effect. Once an inlet was connected with the vertical drainage stack, the other three inlets were sealed. Normally, the top of the vertical drainage stack was open to the outside atmosphere, and the cross-section could be half or fully capped by a plate to change the ventilation conditions. The downstream horizontal pipe was connected to the vertical drainage stack with a 90° elbow joint. The length of the horizontal pipe was 4.00 m with the same diameter as that of the vertical drainage stack. The outlet of the horizontal pipe was inserted into a sink, in which an overflow weir was prepared to control the water level relative to the outlet. Normally, the water level was below the outlet and the water flow was discharged freely. The water level could be controlled by half or fully submerging the outlet.

Water was pumped up to the inflow branch pipe in order to prevent any air entering into the stack through the inlet. The water flow rate (Q_w) was controlled by a valve from 0.4 L/s to 1.6 L/s at an interval of 0.4 L/s and measured by a magnetic flow meter (KROHNE OPTIFLUX 2300C) installed upstream in the inflow pipeline. The

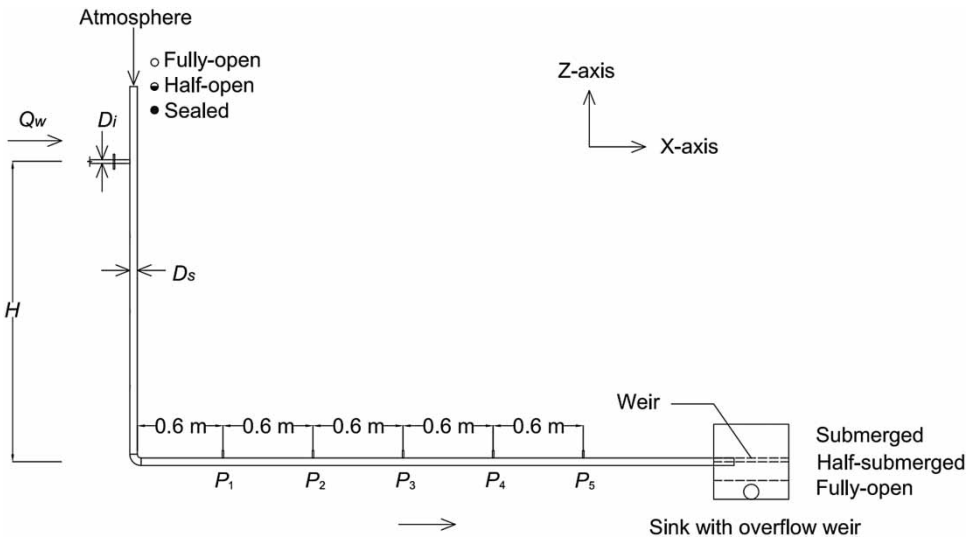

Figure 1 | Schematic diagram of the experimental setup.

magnetic flow meter had an accuracy of 0.2% of its full range (or about 0.08 L/s).

Pressure distribution along the horizontal pipe was measured by five pressure transducers (WESTZH CYB-13). The pressure transducers were installed at the crown of the horizontal pipe to collect the pressure data. The distances between the pressure transducers (P_1, P_2, P_3, P_4 and P_5) and the vertical drainage stack were 0.6 m, 1.2 m, 1.8 m, 2.4 m, and 3.0 m, respectively. The range of the pressure transducers was −2–10 kPa and the accuracy was about 25 Pa. A 60-second sampling time and 100 Hz sampling frequency were set for each experiment to assure adequate test repeatability and accuracy.

A digital video camera (SONY HDR-XR350) positioned about 2.0 m away from the model was used for the visualization of the fluctuation of the water surface and recording of the movement of the air pocket in the horizontal pipe. The videos were taken at a rate of 25 frames per second with a resolution of 1,920 × 1,080 pixels. Images were then extracted from the videos to estimate the water depths by calibrating with the physical scales of the horizontal pipe.

A total of eight experiments were conducted to investigate the pressure variation in the horizontal pipe by combining the four parameters; that is, water flow rate (Q_w), inlet height (H), ventilation condition and outlet condition. Under normal operation condition, the top of the vertical drainage stack and the outlet of the horizontal pipe were fully open to the outside atmosphere. At each inlet height ($H = 0.5$, 1.0, 1.5 and 2.0 m), four water flow rates ($Q_w = 0.4$, 0.8, 1.2 and 1.6 L/s) were tested in turn to simulate different discharge situations. Besides the fully-open ventilation condition, two other ventilation conditions, i.e. half open and sealed, were tested by controlling the plate at the top of the vertical drainage stack. In addition to the fully-open outlet condition, the outlet half-submerged and fully-submerged conditions were tested by controlling the water level relative to the outlet. Table 1 shows the list of experiments. The experiments were conducted at a room temperature of about 20°C.

Table 1 | List of experiments

Exp.	Water flow rate Q_w (L/s)	Inlet height H(m)	Ventilation condition	Outlet condition
1a	0.4, 0.8, 1.2, 1.6[a]	0.5	Fully open	Fully open
1b		1.0		
1c		1.5		
1d		2.0		
2a	0.8	1.5	Half open	Fully open
2b			Sealed	
3a	0.8	1.5	Fully open	Half submerged
3b				Fully submerged

[a]The four water flow rates were tested in turn at each inlet height.

RESULTS AND DISCUSSION

The influences of water flow rate and inlet height

Four water flow rates were tested at each inlet height. All the experiments were under the condition that the top of the vertical drainage stack and the outlet of the horizontal pipe were fully open to the outside atmosphere. Here, experiment 1c (Table 1) was selected as a typical case for analysis.

Ding & Zhu (2018) found that three flow regimes are observed with the increase of the water flow rate in a plunging-type dropshaft: (1) free-flow regime, (2) water-plug regime, and (3) choked regime. The flow regime changes are studied as a function of the dimensionless water flow rate. However, the inflow pipe kept full pipe flow since $Q_w = 0.4$ L/s, so the influence of the inlet was not analyzed in this study. At $Q_w = 0.4$ L/s, the inflow pipe was full pipe flow and the incoming water jet impinged on the opposite sidewall of the vertical drainage stack at a distance below the inlet. After impingement, a central vertical ridge was formed above the impinging point and then the water film flowed down along the sidewall of the vertical drainage stack. With the water dropping down, the air in the vertical drainage stack was entrained moving down. The water flowed down gently along the sidewall. Only a small amount of air bubbles was observed and entrained into the horizontal pipe by the water flow. The bubbles then broke up releasing air into the upper space of the horizontal pipe. The water surface was relatively smooth without significant waves. The collected data from all the pressure transducers fluctuated close to 0 Pa within the accuracy range of 25 Pa.

At $Q_w = 0.8$ L/s, the point of impingement rose up and the water jet splashed above the crown of the inlet. More small air bubbles were observed after the mixture of air and water flow passed through the elbow joint and then the bubbly flow turned into a stratified air-water flow near the measuring point of P_1. In the horizontal pipe, a hydraulic jump was observed near the measuring point of P_2. The

wave reached the crown of the pipe and blocked the air flow above the water surface, resulting in the formation of air pocket. The air pocket was entrained to move downstream by the water flow and a new one was formed upstream. The flow regime could be seen as slug flow. With Q_w increasing to 1.2 L/s and 1.6 L/s, the water jet splashed higher after impingement and the mixture of water and air became more turbulent in the vertical drainage stack. The bubbly flow extended a longer distance before transiting into stratified air-water flow after passing through the elbow joint. Even the measuring point of P_1 was influenced by the bubbly flow. In the horizontal pipe, the water surface rose up with Q_w increasing and the section of water column between air pockets got longer.

The temporal response of pressure fluctuation at P_1, P_2, P_3, P_4, and P_5 in experiment 1c was monitored at $Q_w =$ 0.8 L/s. Strong pressure oscillations were observed at all measuring points. The pressure fluctuated at an average value of 231 Pa with an amplitude of 181 Pa at P_1, 204 Pa with an amplitude of 173 Pa at P_2, 105 Pa with an amplitude of 196 Pa at P_3, 71 Pa with an amplitude of 187 Pa at P_4, and 48 Pa with an amplitude of 158 Pa at P_5. The air entrained from the upstream vertical drainage stack was blocked by the hydraulic jump in the horizontal pipe, so a positive pressure zone was formed at the elbow joint. Considering P_1 was the nearest to the elbow joint, the average pressure of P_1 was the largest. With the water flowing downstream, the pressure decreased along the horizontal pipe until the outlet where the pressure was atmospheric. Therefore, the pressure in the horizontal pipe was mainly positive. Notice that the amplitudes of the pressure fluctuation along the horizontal pipe changed

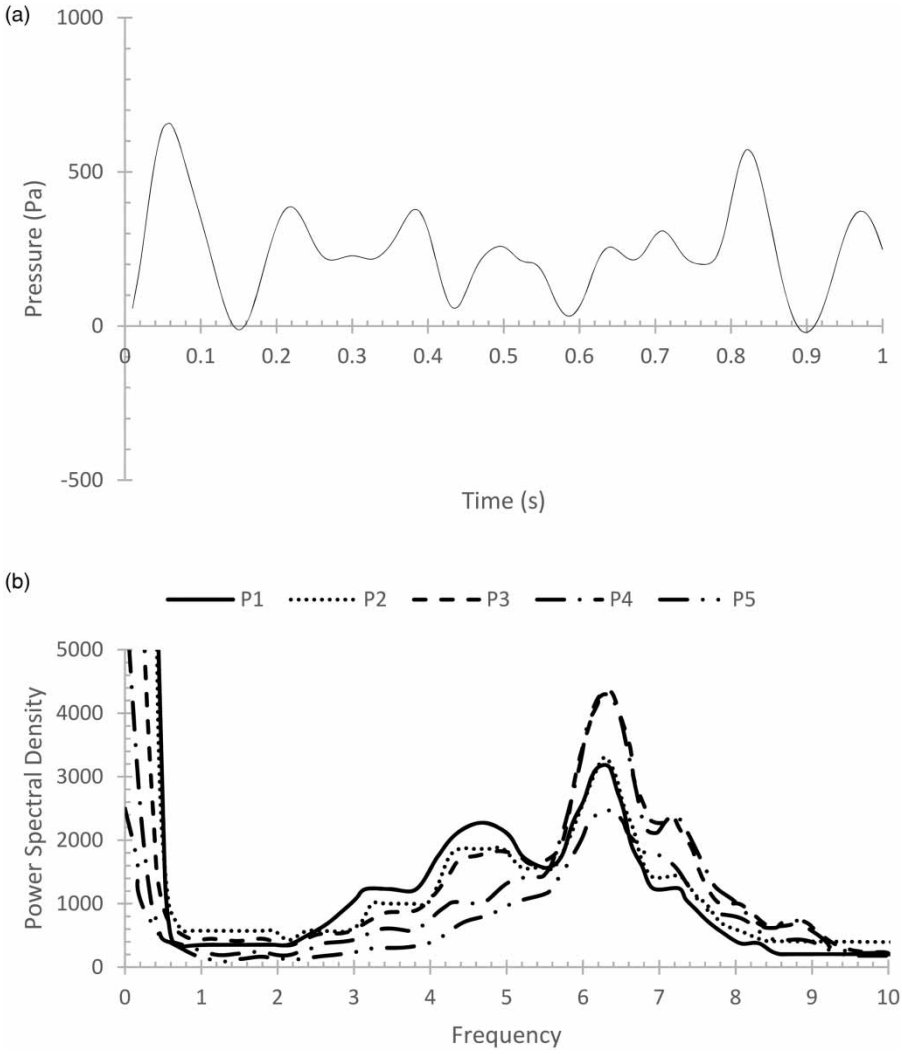

Figure 2 | (a) Pressure fluctuation at P_1 in 1 second and (b) frequency spectrum at P_1, P_2, P_3, P_4, and P_5 in Exp. 1c ($Q_w = 0.8$ L/s, $H = 1.50$ m, fully-open top and outlet).

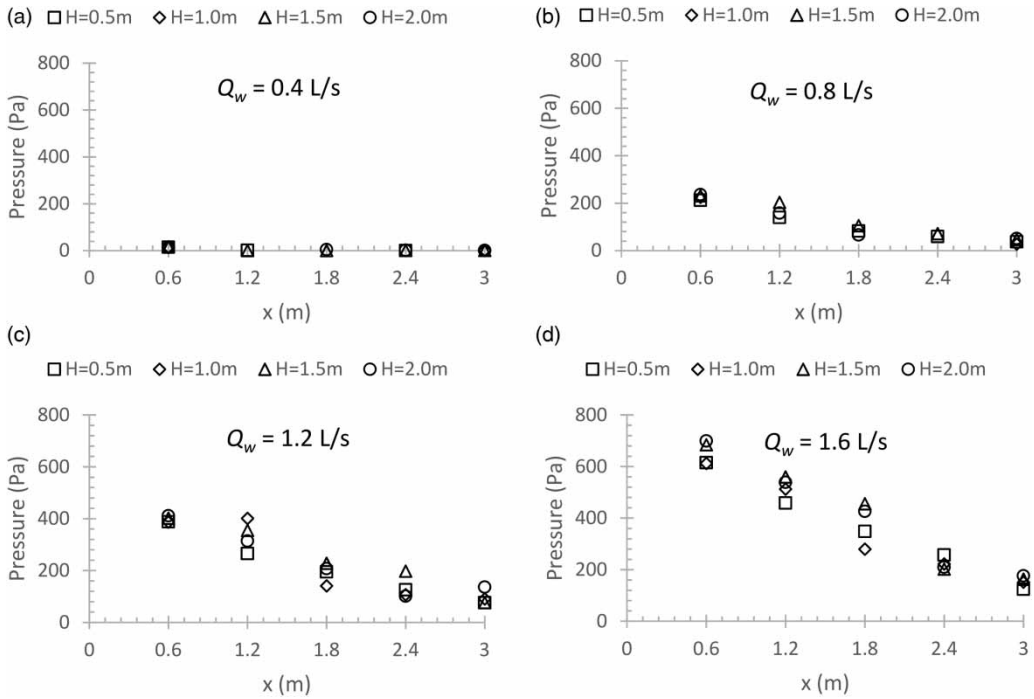

Figure 3 | Average pressure variation along the horizontal pipe at different water flow rate Q_w and inlet height H in Exp. 1a, 1b, 1c and 1d (fully-open top and outlet).

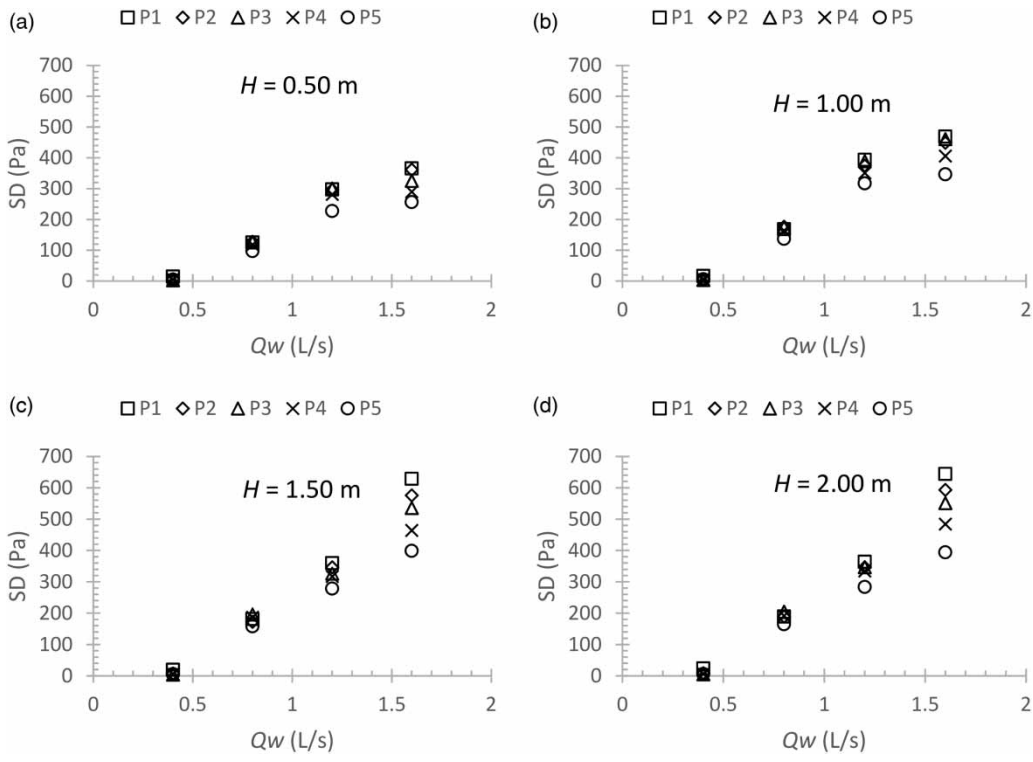

Figure 4 | Standard deviation of pressure at different water flow rate Q_w and inlet height H in Exp. 1a, 1b, 1c and 1d (fully-open top and outlet).

little compared with the mean value of the pressure, which will be discussed later.

Figure 2(a) shows a detailed pressure fluctuation where the frequency of the pressure fluctuation was about 7 Hz, which was consistent with Fourier analysis of its frequency, as shown in Figure 2(b). Figure 2(b) shows the power spectral density of the data from the five pressure transducers. It can be seen that the characteristic frequencies at different measuring points were similar along the horizontal pipe. In the frequency spectrum, there were two characteristic frequencies, 0 Hz for the average pressure and 7 Hz for the pressure fluctuation. At the upstream zone of the horizontal pipe, for example P_1, the power spectral density of 0 Hz was much larger than that of 7 Hz, which meant the average pressure played an important role in the pressure variation. As mentioned before, with the water flowing downstream along the horizontal pipe, the average pressure value decreased while the pressure fluctuation did not change much, so the influence of pressure fluctuation on pressure variation compared with the average pressure value gradually became obvious at the downstream zone of the horizontal pipe, for example P_5.

Considering the water was supplied steadily, the position of water trap seal was mainly maintained by the average pressure. Therefore, in this study the mean value of pressure was adopted to judge if the pressure in the horizontal pipe exceeded the safety range of the water trap seal. Figure 3 shows the average pressure variation along the horizontal pipe at different Q_w and inlet height H in experiment 1a, 1b, 1c and 1d. The X-axis was the distance from the measuring point to the vertical drainage stack. From the figure it can be seen that the influence of water flow rate on the pressure variation was similar at different inlet heights. At $Q_w = 0.4$ L/s, as it was free surface flow in the horizontal pipe, the upper part of the pipe was connected with the outside atmosphere directly. The pressure data at all measuring points were close to atmospheric pressure. From $Q_w = 0.8$ L/s on, the free surface flow turned into slug flow. The air at the upper part was blocked by the water slug. As the air entrained into the horizontal pipe could not be discharged directly, it was compressed by the surrounding water, which resulted in the pressure increase. With the water flow rate increasing, the average pressures at different measuring points increased correspondingly. As P_1 was the nearest to the positive pressure zone, the largest pressure was always collected at P_1. Then the pressure decreased along the horizontal pipe. As the pressure at the outlet was atmospheric, the pressure variation was mainly determined by the upstream positive pressure. Figure 4 shows the standard deviation of the pressure at different Q_w and inlet height H in experiment 1a, 1b, 1c and 1d. By comparing the curves at a certain inlet height, it can be seen that the increase tendencies of the pressure standard deviation at different measuring points were similar. The differences in the standard deviations of pressure gradually became obvious with the water flow rate increasing. Therefore, the pressure variation in the horizontal pipe is mainly determined by the water flow rate, while the effect of inlet height on the pressure variation appears to be less significant.

The influence of ventilation condition

In building drainage and vent systems, the falling water flow would entrain the air in the vertical drainage stack. As mentioned above, when the top of the vertical drainage stack was fully open, a mixture flow of air and water was formed in the vertical drainage stack, as shown in Figure 5(a). Even if the top was half covered by a plate, enough air could be continuously supplied into the vertical drainage stack. So, the flow regimes under fully-open and

Figure 5 | Flow regimes in the vertical stack for (a) top fully-open condition in Exp. 1c and (b) top sealed condition in Exp. 2b ($Q_w = 0.8$ L/s, H = 1.50 m, fully-open outlet).

half-open conditions were nearly the same. Once the top of the vertical drainage stack was totally sealed, air could not enter the system through the top of the vertical drainage stack. With the air residual in the vertical drainage stack being entrained away into the horizontal pipe, a negative pressure zone was formed firstly at the top of the vertical drainage stack and extended down gradually to the bottom. An air-water mixed plug started to form at the bottom of the vertical drainage stack above the elbow joint. During this process, the residual air in the vertical drainage stack was entrained by the turbulent surface of the water plug and then transported into the downstream horizontal pipe. For the lack of air supplement, the water plug was choked up and finally submerged the crown of the inlet. As no air was supplied into the vertical drainage stack, the turbulent mixture of water and air gradually turned into a full pipe flow with small air bubbles, as shown in Figure 5(b). After passing through the elbow joint, a full pipe flow with small air pockets was observed in the horizontal pipe.

Figure 6 shows the average pressure variation along the horizontal pipe under different ventilation conditions at the top of the vertical drainage stack in experiment 1c, 2a and 2b. Three ventilation conditions; that is, top fully open, half open and sealed, were tested at $Q_w = 0.8$ L/s and $H =$ 1.5 m. It can be seen that the pressure variations in the horizontal pipe were nearly the same under the top fully-open and half-open conditions while the pressure distribution decreased by about 51 Pa under the top-sealed condition. Under the top-sealed condition, for the reason of frictional head loss, the pressure drop along the horizontal pipe was about 64.9 Pa/m. The downstream atmospheric outlet mainly determined the pressure variation in the horizontal pipe. So P_5 was close to 0 Pa. Notice that the amplitude of the pressure fluctuation under the top-sealed condition was much smaller than those under the top fully-open and half-open conditions. The mean pressure and the pressure fluctuation were both small in the horizontal pipe under the top-sealed condition, and the negative pressure in the vertical drainage pipe could cause the breakup of the

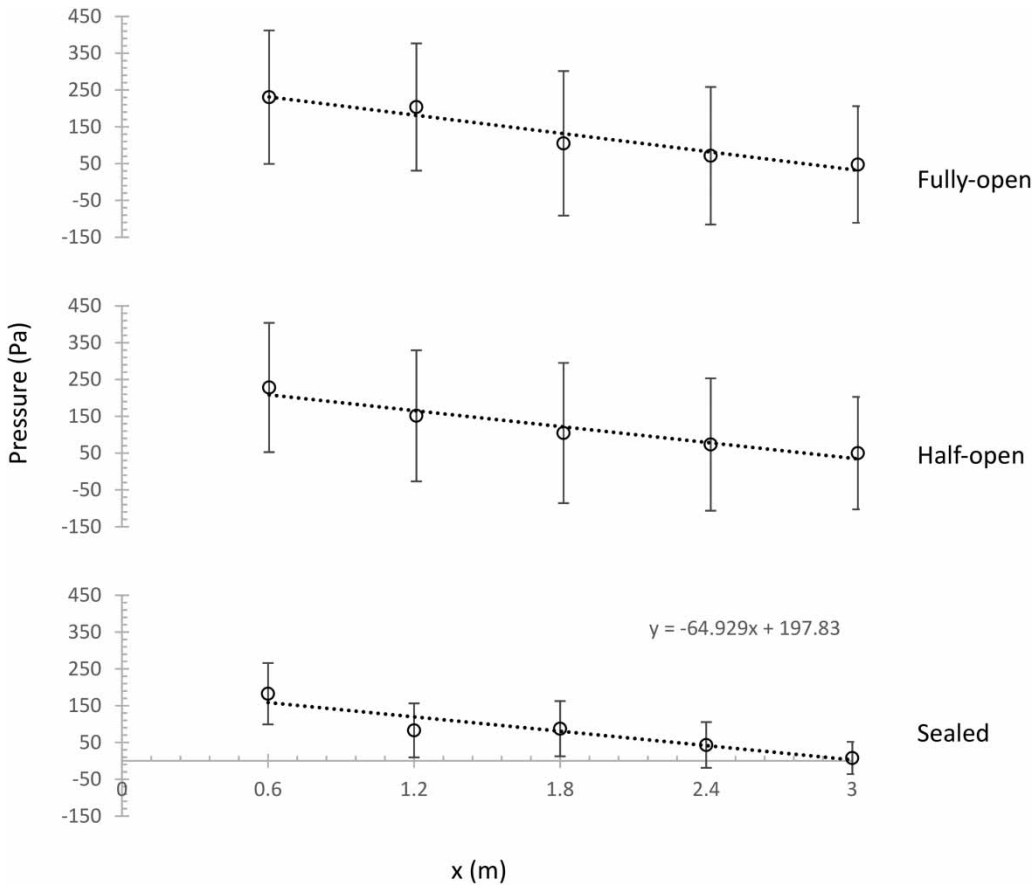

Figure 6 | Average pressure variation along the horizontal pipe under different ventilation conditions in Exp. 1c, 2a and 2b ($Q_w = 0.8$ L/s, H = 1.50 m, fully-open outlet).

water trap seal in the branch pipes, which should be avoided in actual operation.

The influence of outlet condition

In an actual building drainage and vent system, the outlet of the horizontal pipe is usually fully open to the atmosphere above the water surface. If downstream water is not discharged away in time by some excessive or inadvertent event temporarily, the outlet would be submerged by the ponded water. In this experiment, a plexiglas plate was used as an overflow weir to simulate the outlet half-submerged condition. Similarly, the outlet fully-submerged condition was simulated by raising the water level to the crown of the outlet pipe.

Figure 7 shows the average pressure variation along the horizontal pipe under different outlet conditions in experiment 1c, 3a and 3b. Three outlet conditions; that is, fully open, half submerged and fully submerged, were tested at $Q_w = 0.8$ L/s and $H = 1.5$ m. From the figure, it can be seen that the pressure variations in the horizontal pipe were nearly the same under the outlet fully-open and half-submerged conditions while the pressure variation significantly increased by about 652 Pa under the outlet fully-submerged condition. The flow regime in the horizontal pipe under the outlet fully-open condition was slug flow. When the outlet was half submerged, the upper part of the pipe was not blocked by the water in the sink. So, the flow regime was similar to that under the outlet fully-open condition. The air pocket could be entrained and discharged freely. The pressure distributions were nearly the same under the outlet fully-open and half-submerged conditions. When the outlet was submerged, the outlet of the horizontal pipe was blocked by the water, and the air pocket in the horizontal pipe could not be entrained and discharged freely. Meanwhile, the upstream incoming flow would compress the air-water mixture in the horizontal pipe. Therefore, the average pressure in the horizontal pipe was significantly higher than that under the outlet fully-open and half-submerged conditions. The pressure drop under the outlet fully-submerged condition was about 64.8 Pa/m, which was very close to that under the top-sealed condition. Notice that the error bar of pressure under the outlet-submerged condition was much larger than those under the outlet fully-open and half-submerged conditions, which meant the pressure fluctuation under the outlet fully-submerged condition was quite larger. The

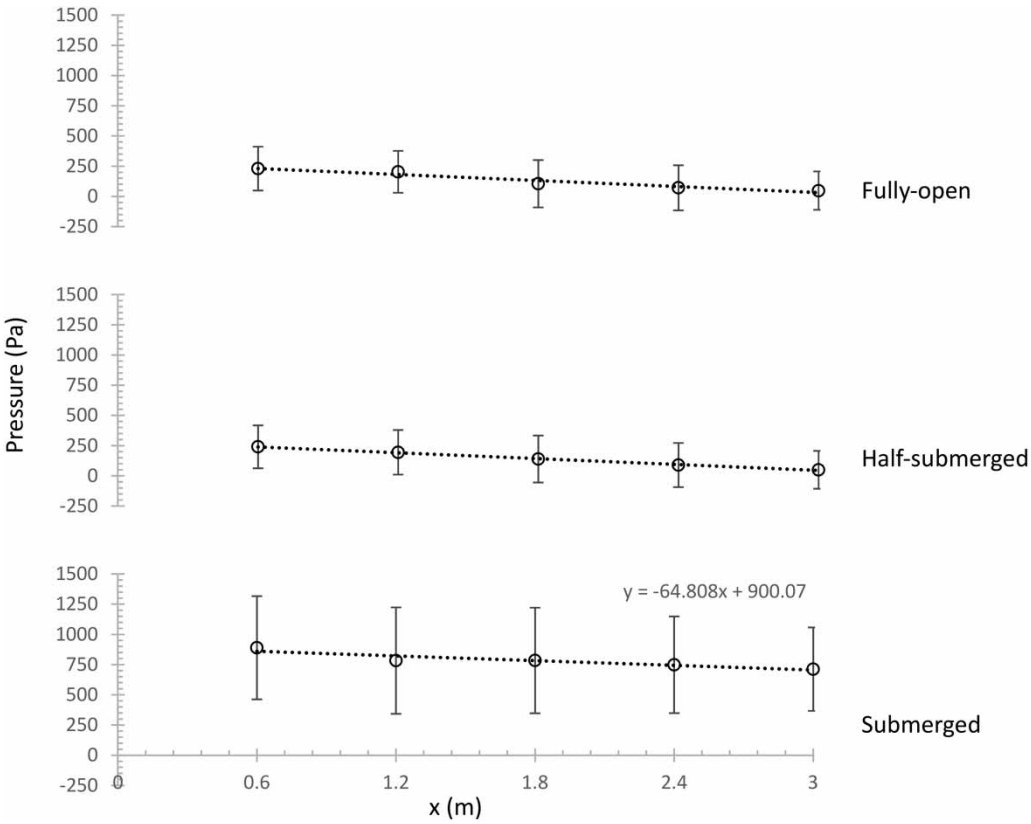

Figure 7 | Average pressure variation under different outlet conditions along the horizontal pipe in Exp. 1c, 3a and 3b ($Q_w = 0.8$ L/s, H = 1.50 m, fully-open top).

positive pressure increase caused by the outlet submergence must be avoided in the actual operation.

Air entrainment

As mentioned before, the water flow would entrain air into the horizontal pipe to form an air-water two-phase slug flow. The characteristics of air pockets such as their length, height and volume were obtained from digital video images. The air flow rate Q_a and water flow rate Q_w were then estimated. Figure 8(a) shows the schematic diagram of the air-water two-phase slug flow. According to the images extracted by frame from the videos, the cross-sectional areas of air pocket A_1 and water column under the air pocket A_2 were calculated. The air flow rate Q_a and water flow rate Q_w were estimated as:

$$Q_a = \frac{\Sigma(A_1 \cdot l_1)}{T} \quad (1)$$

$$Q_w = \frac{\Sigma[A_2 \cdot l_1 + (A_1 + A_2) \cdot l_2]}{T} \quad (2)$$

Here, experiment 1c with $H = 1.5$ m, fully-open top and outlet was selected as a typical example to calculate Q_a. Notice that the free surface flow at $Q_w = 0.4$ L/s was not calculated for the reason that no air pocket was yet formed then. The relative air flow rate Q_a/Q_w was calculated and compared with the results of Rajaratnam *et al.* (1997). In the figure, the water flow rate Q_w was expressed in terms of a dimensionless flow rate Q^* defined by the equation $Q^* = Q_w/(gD_s^5)^{1/2}$, which was helpful to discuss from particular configuration to general application. The relative air flow rate was about 0.3 in this experiment, while Rajaratnam *et al.* (1997) reported that the relative air flow rate decreased from about 1 to 0.4 when the flow rate increased, as shown in Figure 8(b).

SUMMARY AND CONCLUSIONS

The paper presents an experimental study on the air pressure variation in a horizontal pipe of a single-stack drainage system. The relationships between the pressure

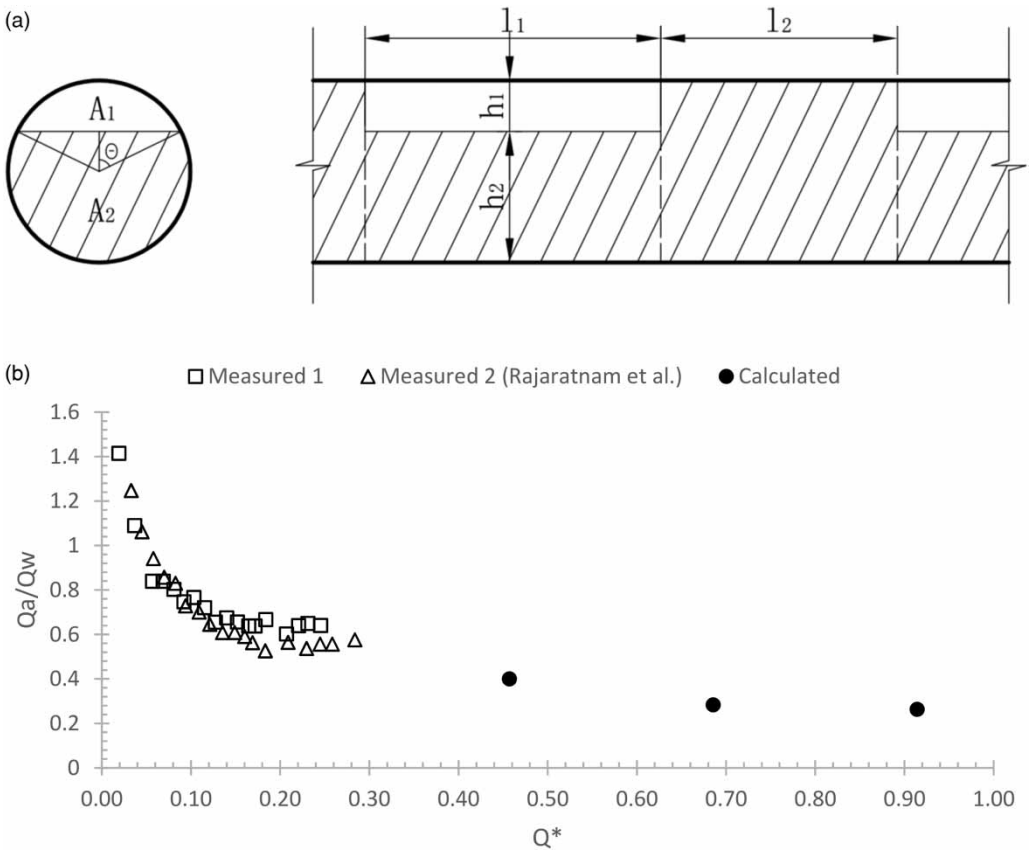

Figure 8 | (a) Schematic diagram of air-water two-phase slug flow and (b) relative air flow rate Q_a/Q_w with Q* in experiment 1c (H = 1.50 m, fully-open top and outlet).

variation and four parameters, i.e. water flow rate, inlet height, ventilation condition and outlet condition were studied. The following main results are found:

(1) At a certain inlet height, with the water flow rate increasing, the mean values and magnitudes of pressure fluctuation at all measuring points increased. The pressure decreases along the horizontal pipe from the elbow joint with positive pressure to the atmospheric outlet.
(2) The inlet height has not much influence on the pressure variation in the horizontal pipe.
(3) The ventilation condition at the top of the vertical drainage stack could influence the flow regime in the vertical drainage stack, which would change the pressure variation in the horizontal pipe. When the top of the vertical drainage stack was sealed, a full pipe flow with small air bubbles in the vertical drainage stack and the horizontal drainage pipe could be formed at a large flow rate. The pressure values and pressure fluctuations in the horizontal drainage pipe are relatively small.
(4) The outlet condition could influence the flow regime in the horizontal pipe. If the outlet was not totally submerged, the air pocket in the horizontal pipe could be entrained and discharged freely, and there was not much difference in the pressure variation in the horizontal pipe. Once the outlet was completely submerged, the positive pressure would increase sharply, which should be avoided in the actual operation.

This study highlighted that the water flow rate determines the pressure variation in the horizontal pipe while the inlet height had little influence on the pressure variation. Meanwhile, the upstream ventilation condition at the top of the vertical drainage stack and the downstream outlet condition should be paid attention to avoid excessive pressure variation. The diameter, the length, and the elbow amount of the horizontal pipe should be carefully designed to ensure the safety of building drainage and vent system.

ACKNOWLEDGEMENTS

The authors gratefully acknowledge the financial support from National Science and Technology Major Projects for Water Pollution Control and Treatment (2017ZX07201003), National Key Research and Development Plan (2016YFC04006) and Science and Technology Program of Zhejiang Province (2015C33007). The authors are also thankful for Mr Guogui Liu of Institute of Municipal Engineering, Zhejiang University for the setup of the experimental model and his technical assistance during the experimental work.

REFERENCES

Chanson, H. 2009 Turbulent air-water flows in hydraulic structures: dynamic similarity and scale effects. *Environmental Fluid Mechanics* **9** (2), 125–142.

Cheng, C. L., Lu, W. H. & Shen, M. D. 2005 An empirical approach: prediction method of air pressure distribution on building vertical drainage stack. *Journal of the Chinese Institute of Engineers* **28** (2), 205–217.

Cheng, C. L., Yen, C. J., Lu, W. H. & He, K. C. 2008a An empirical approach to determine peak air pressure within the 2-pipe vertical drainage stack. *Journal of the Chinese Institute of Engineers* **31** (2), 199–213.

Cheng, C. L., Yen, C. J., Wong, L. T. & Ho, K. C. 2008b An evaluation tool of infection risk analysis for drainage systems in high-rise residential buildings. *Building Services Engineering Research and Technology* **29** (3), 233–248.

Ding, Q. & Zhu, D. Z. 2018 Flow regimes in a dropshaft with limited air supply. *Journal of Hydraulic Engineering* **144**, 5.

Huang, B., Wu, S. Q., Zhu, D. Z. & Schulz, H. E. 2018 Experimental study of geysers through a vent pipe connected to flowing sewers. *Water Science and Technology* **2017** (1), 66–76.

Kay, D., Watkins, J. & Fewtrell, L. 2006 An evaluation of public health issues associated with, or arising from, drainage-based infection spread. *Building Services Engineering Research and Technology* **27** (2), 119–125.

Kelly, D. A., Swaffield, J. A., Jack, L. B., Campbell, D. P. & Gormley, M. 2008a Pressure transient identification of depleted appliance trap seals: a pressure pulse technique. *Building Services Engineering Research and Technology* **29** (2), 165–181.

Kelly, D. A., Swaffield, J. A., Jack, L. B., Campbell, D. P. & Gormley, M. 2008b Pressure transient identification of depleted appliance trap seals: a sinusoidal wave technique. *Building Services Engineering Research and Technology* **29** (3), 219–232.

Li, L. & Zhu, D. Z. 2018 Modulation of the transient pressure by an air pocket in a horizontal pipe with an end orifice. *Water Science and Technology* **77** (10), 2528–2536.

Ma, Y. Y., Zhu, D. Z. & Rajaratnam, N. 2016 Air entrainment in a tall plunging flow dropshaft. *Journal of Hydraulic Engineering* **142** (10), 04016038.

Qian, Y., Zhu, D. Z. & Edwini-Bonsu, S. 2018 Air flow modeling in a prototype sanitary sewer system. *Journal of Environmental Engineering* **144** (3), 04018008.

Rajaratnam, N., Mainali, A. & Hsung, C. Y. 1997 Observations on flow in vertical dropshafts in urban drainage systems. *Journal of Environmental Engineering* **123** (5), 486–491.

Stephenson, D. & Metcalf, J. R. 1991 Model studies of air entrainment in the Muela drop shaft. *Proceedings of the Institution of Civil Engineers* **91** (3), 417–434.

Swaffield, J. A. & Campbell, D. P. 1992 Air pressure transient propagation in building drainage vent systems, an application of unsteady flow analysis. *Building and Environment* **27** (3), 357–365.

Swaffield, J. A. & Jack, L. B. 1998 Drainage vent systems: investigation and analysis of air pressure regime. *Building Services Engineering Research and Technology* **19** (3), 141–148.

Swaffield, J. A. & Jack, L. B. 2004 Simulation and analysis of airborne cross-contamination routes due to the operation of building drainage and vent systems. *Building Research and Information* **32** (6), 451–467.

Swaffield, J. A. & Thancanamootoo, A. 1991 Modelling unsteady annular downflow in vertical building drainage stacks. *Building and Environment* **26** (2), 137–142.

Swaffield, J. A., Jack, L. B. & Campbell, D. P. 2004a Control and suppression of air pressure transients in building drainage and vent systems. *Building and Environment* **39** (7), 783–794.

Swaffield, J. A., Jack, L. B., Campbell, D. P. & Gormley, M. 2004b Positive air pressure transient propagation in building drainage and vent systems. *Building Services Engineering Research and Technology* **25** (2), 77–88.

Wang, Y. C., Nobi, N., Nguyen, T. & Vorreiter, L. 2012 A dynamic ventilation model for gravity sewer networks. *Water Science and Technology* **65** (1), 60.

Wei, J., Ma, Y., Zhu, D. Z. & Zhang, J. 2018 Effect of boundary conditions on the performance of a dropshaft with an internal divider. *Water Science and Technology* **2017** (2), 441–449.

First received 1 August 2018; accepted in revised form 3 January 2019. Available online 10 January 2019